# Influence of nuclear basic data on the calculation of production cross sections of superheavy nuclei

X. J. Bao (包小军),[1] Y. Gao (高远),[2] J. Q. Li (李君清),[1,3] and H. F. Zhang (张鸿飞)[1,*]

[1]*School of Nuclear Science and Technology, Lanzhou University, 730000 Lanzhou, People's Republic of China*

[2]*School of Information Engineering, Hangzhou Dianzi University, Hangzhou 310018, People's Republic of China*

[3]*Institute of Modern Physics, Chinese Academy of Science, Lanzhou 730000, People's Republic of China*

(Received 26 April 2015; published 1 July 2015)

The center of the predicted island of stability of superheavy nuclei (SHN) has not yet been observed experimentally. Many theories are being developed to understand the synthesizing mechanism of superheavy nuclei. However, all of them have to use some basic nuclear data. Three data tables, FRDM1995 [P. Möller *et al.*, At. Data Nucl. Data Tables **59**, 185 (1995)], KTUY2005 [H. Koura *et al.*, Prog. Theor. Phys. **113**, 305 (2005)], and WS2010 [Ning Wang *et al.*, Phys. Rev. C **82**, 044304 (2010)], are used to investigate the SHN production. Based on the dinuclear system concept, the evaporation residue cross sections of SHN for $Z$=112–118 are calculated for the $^{48}$Ca-induced hot fusion reactions. It turns out that unlike the predictions made with the KTUY2005 and WS2010 data, the magic numbers $Z$=114 and $N$=184 predicted with the FRDM1995 data do not contradict the experimental data obtained so far.

DOI: 10.1103/PhysRevC.92.014601 PACS number(s): 27.90.+b, 25.70.Jj, 24.10.Nz, 25.70.Gh

## I. INTRODUCTION

Since the "island of stability" was predicted theoretically [1–5], great success has been achieved during the past two decades experimentally. Up to now, the superheavy nuclei (SHN) $Z$=107–118 have been synthesized in the laboratory by fusion reactions [6–11]. However, the exact position of the island of stability has not yet been observed by experiments. To fulfill the task, one has to further understand the synthesizing mechanism, and many theoretical models are being developed [12–25]. To precisely reproduce the experimental data, all the models meet the same problems, one of which is that the basic nuclear data such as the masses and deformations of colliding nuclei, the light particle separation energy, and the fission barrier must be reliable to some extent. Presently we are concerned with three groups of the theoretically calculated data. The FRDM95 data by Möller *et al.* [26], which are composed of macroscopic droplet terms and a microscopic shell correction terms. The macroscopic term is calculated using the finite-range droplet model (FRDM), while the shell term is calculated using the folded-Yukawa single-particle potential, which is widely used. The Weizsaecker-Skyrme (WS2010) table [27] is also based on a macroscopic-microscopic method, in which the isospin and mass dependence of model parameters including axial deformation are investigated with the Skyrme energy density functional together with the extended Thomas-Fermi approximation. The shell correction term is calculated using the Woods-Saxon single-particle potential. The Koura-Tachibana-Uno-Yamada (KTUY2005) group's mass formula [28] is composed of two parts: one representing the general trend of the masses as a function of the proton and neutron numbers ($Z$, $N$), and the other representing the deviations from this general trend. The latter is caused by the shell structure and the deformation of the nucleus. Recently Sobiczewski and Litvinov [29] have provided a quantitative test of the ability of several models (covering the FRDM1995, KTUY2005, and WS2010) to predict nuclear masses. That paper concludes that for most of the models, the accuracy improves when passing from lighter nuclei to heavier ones. That is to say, for predicting the masses of the SHN the power of the nuclear mass models can reach a higher accuracy. It demonstrated that for heavy nuclei $Z > 82$ the rms value reduced to 0.179 (WS2010), 0.448 (FRDM1995), 0.869 (KTUY2005) MeV, respectively.

Based on the dinuclear system (DNS) model, the evaporation residue cross sections (ERCSs) to produce SHN are calculated here by using the above three nuclear data tables to see their application effect on the ERCSs. The paper is organized as follows. In the Sec. II, we introduce the general formalism of the DNS model in order to explicitly show each term and how it is related to the nuclear basic data. The numerical results are presented and discussed in Sec. III. First, the survival probabilities of SHN with charge numbers $Z$=112–118 in the $xn$-evaporation channels are extracted from the experimental ERCSs, then in the framework of the DNS model the stability of the SHN is checked, since different theoretical models have predicted different positions of the island of stability of SHN. Finally, a brief summary of the results is given in Sec. IV.

## II. THEORETICAL FRAMEWORK

First, we introduce the general formalism of the DNS model in order to explicitly show each term and how it is related to the nuclear basic data. In the DNS concept, the ERCS is expressed as [16,30–32]

$$\sigma_{\rm ER}(E_{\rm c.m.}) = \frac{\pi\hbar^2}{2\mu E_{\rm c.m.}} \sum_J (2J+1) T(E_{\rm c.m.}, J) \times P_{\rm CN}(E_{\rm c.m.}, J) W_{\rm sur}(E_{\rm c.m.}, J), \quad (1)$$

where $E_{\rm c.m.}$ is the center-of-mass incident energy, and $T(E_{\rm c.m.}, J)$ is the transmission probability of the projectile overcoming the potential barrier to form a DNS. $P_{\rm CN}(E_{\rm c.m.}, J)$

*zhanghongfei@lzu.edu.cn

 

is the probability that the system evolves from a touching configuration to a compound nucleus in competition with quasifission. The last term is the survival probability of the formed excited compound nucleus [33]. The sum is over all partial waves $J$.

### A. Capture cross section and transmission probability

The capture cross section is

$$\sigma_{\rm cap}(E_{\rm c.m.}) = \frac{\pi\hbar^2}{2\mu E_{\rm c.m.}}\sum_J (2J+1)T(E_{\rm c.m.},J), \qquad (2)$$

where the transmission probability can be written as

$$T(E_{\rm c.m.},J) = \int f(B)\frac{1}{1+\exp\left\{-\frac{2\pi}{\hbar\omega(J)}\left[E_{\rm c.m.}-B-\frac{\hbar^2}{2\mu R_B^2}J(J+1)\right]\right\}}dB, \qquad (3)$$

where $\hbar\omega(J)$ is the width of the parabolic Coulomb barrier at the position $R_B(J)$, and an empirical coupled channel method is used via a barrier distribution function which is taken as an asymmetric Gaussian form $f(B) = \frac{1}{N}\exp[-(\frac{B-B_m}{\Delta_1})^2](B < B_m)$ and $f(B) = \frac{1}{N}\exp[-(\frac{B-B_m}{\Delta_2})^2](B > B_m)$ with $B_m = (B_0+B_s)/2$ as mentioned in Ref. [15]. $B_0$ and $B_s$ are the height of the Coulomb barrier at waist-to-waist orientation and the height of the minimum barrier with variance of dynamical deformation $\beta_1$ and $\beta_2$, respectively. $N$ is the normalization constant. The nucleus-nucleus interaction potential with quadrupole deformation is taken as the form

$$V(r,\beta_1,\beta_2,\theta_1,\theta_2) = V_C(r,\beta_1,\beta_2,\theta_1,\theta_2) + V_N(r,\beta_1,\beta_2,\theta_1,\theta_2) + \tfrac{1}{2}C_1\left(\beta_1-\beta_1^0\right)^2 + \tfrac{1}{2}C_2\left(\beta_2-\beta_2^0\right)^2. \qquad (4)$$

The nuclear potential and Coulomb potential are taken as the forms in Ref. [34]:

$$V_N(r,\beta_1,\beta_2,\theta_1,\theta_2) = -V_0\left[1+\exp\left(r-\sum_{i=1}^{2}R_i\left[1+(5/4\pi)^{1/2}\beta_i P_2(\cos\theta_i)\right]/a\right)\right], \qquad (5)$$

and

$$V_C(r,\beta_1,\beta_2,\theta_1,\theta_2) = \frac{Z_1Z_2e^2}{r} + \left(\frac{9}{20\pi}\right)^{1/2}\left(\frac{Z_1Z_2e^2}{r^3}\right)\times\sum_{i=1}^{2}R_i^2\beta_i P_2(\cos\theta_i) + \left(\frac{3}{7\pi}\right)\times\left(\frac{Z_1Z_2e^2}{r^3}\right)\sum_{i=1}^{2}R_i^2[\beta_i P_2(\cos\theta_i)]^2. \qquad (6)$$

Here $\theta_i$ is the angle between the symmetry axis of the $i$th nucleus and the collision axis. $\beta_i$ and $R_i$ are the quadrupole deformation parameter and radius of the $i$th nucleus, respectively. The strength $V_0$ and the diffusion width $a$ of the nuclear potential are set to be 80.0 MeV and 0.68 fm, respectively.

### B. Fusion probability

The fusion probability is obtained by numerically solving a set of master equations (MEs) with the neutron and proton numbers of the projectilelike fragment being variables, and also the variables in the corresponding potential energy surface [35,36]. The distribution probability function, $P(Z_1,N_1,E_1,t)$, at time $t$ to find $Z_1$ protons and $N_1$ neutrons in fragment 1 with excitation energy $E_1$, obeys the following master equation:

$$\frac{dP(Z_1,N_1,E_1,t)}{dt} = \sum_{Z_1'}W_{Z_1,N_1;Z_1',N_1}(t)\left[d_{Z_1,N_1}P(Z_1',N_1,E_1',t)w - d_{Z_1',N_1}P(Z_1,N_1,E_1,t)\right] + \sum_{N_1'}W_{Z_1,N_1;Z_1,N_1'}(t)\times\left[d_{Z_1,N_1}P(Z_1,N_1',E_1',t) - d_{Z_1,N_1'}P(Z_1,N_1,E_1,t)\right] - [\Lambda_{\rm qf}(\Theta(t)) + \Lambda_{\rm fs}(\Theta(t))]P(Z_1,N_1,E_1,t), \qquad (7)$$

where $W_{N_1,Z_1;N_1',Z_1}$ is the mean transition probability from channel $(N_1',Z_1,E_1')$ to $(N_1,Z_1,E_1)$, while $d_{N_1,Z_1}$ denotes microscopic dimensions corresponding to the macroscopic state $(N_1,Z_1,E_1)$. The sum is taken over all possible proton and neutron numbers that fragment $Z_1'$, $N_1'$ may take, but only one nucleon transfer is considered in the model with $Z_1' = Z_1 \pm 1$ and $N_1' = N_1 \pm 1$. The excitation energy $E_1$ is determined by the dissipation energy from the relative motion [37,38] and the potential energy surface (PES) of the DNS. The motion of nucleons in the interacting potential is governed by the single-particle Hamiltonian, and the interaction. The evolution of the DNS along the distance between nuclei $R$ leads to the quasifission. The quasifission rate $\Lambda_{\rm qf}$ and fission rate (for heavy fragment) $\Lambda_{\rm fs}$ are estimated with the one-dimensional Kramers formula [39,40].

In the relaxation process of the relative motion, the nuclei are excited by the dissipation of the relative kinetic energy. The local excitation energy is determined by this transferred excitation energy of the composite system and the PES of the DNS. The PES is given by

$$U(N_1,Z_1,N_2,Z_2,R,\beta_1,\beta_2,J) = B(N_1,Z_1,\beta_1) + B(N_2,Z_2,\beta_2) - [B(N,Z,\beta) + V_{\rm rot}^{\rm CN}(J)] + U_C(Z_1,Z_2,\beta_1,\beta_2,R) + U_N(N_1,Z_1,N_2,Z_2,R,\beta_1,\beta_2,J), \qquad (8)$$

where $N = N_1+N_2$ and $Z = Z_1+Z_2$. $\beta_i(i=1,2)$ and $\beta$ represent the quadrupole deformation of the two fragments and compound nucleus, respectively. $R$ is the distance between nuclei at which the interaction potential between the two

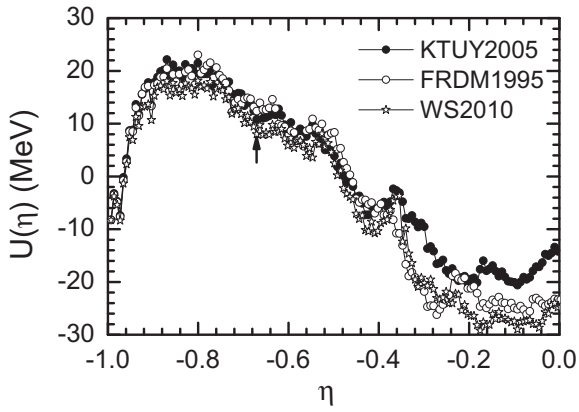


FIG. 1. The PES for the reaction $^{48}$Ca+$^{243}$Am as a function of mass asymmetry $\eta$ based on different nuclear mass tables.

nuclei $U_C + U_N$ has the minimum value. The $B(N_1,Z_1,\beta_1)$, $B(N_2,Z_2,\beta_2)$, and $B(N,Z,\beta)$ are the binding energies of two deformed nuclei and compound nucleus, respectively. $U_C(Z_1,Z_2,\beta_1,\beta_2,R)$, $U_N(N_1,Z_1,N_2,Z_2,R,\beta_1,\beta_2,J)$, and $V_{\rm rot}^{\rm CN}(J)$ are the nuclear, Coulomb interaction potential, and the centrifugal energy, respectively. The Coulomb interaction can be calculated with Wong's formula [34], and the nuclear potential is calculated with Skyrme-type interaction without considering the momentum and spin dependence (see Ref. [41] and references therein).

The PES (the driving potential for nucleon transfer) should be $Z_1$ and $N_1$ dependent; however, for a certain reaction system such as $^{48}$Ca+$^{243}$Am, the entrance point is in the valley of the two-variable driving potential due to the double magic projectile $^{48}$Ca. The driving potential along the valley can be described as a function of the mass asymmetry $\eta = (A_1 - A_2)/(A_1 + A_2)$ and is displayed in Fig. 1 based on different nuclear tables. The arrow in the figure indicates the entrance channel $\eta_i$. One may find that the PES shifts from one to another, so that not only the potential energies at the injection point are different, but also different are the highest energies of the potential from different nuclear tables. This means different inner fusion barriers. And there are differences in the symmetric region.

The compound nucleus formation probability at the Coulomb barrier $B$, which corresponds to a certain orientation of the colliding nuclei in the entrance channel, and for the angular momentum $J$ is given by

$$P_{\rm CN}(E_{\rm c.m.},J,B) = \sum_{Z_1=1}^{Z_{\rm BG}} \sum_{N_1=1}^{N_{\rm BG}} P(Z_1,N_1,E_1,\tau_{\rm int}). \qquad (9)$$

The interaction time $\tau_{\rm int}$ in the dissipative process of two colliding nuclei is dependent on the incident energy $E_{\rm c.m.}$, $J$, and $B$, and is determined by using the deflection function method [22]. We obtain the fusion probability as

$$P_{\rm CN}(E_{\rm c.m.},J) = \int f(B) P_{\rm CN}(E_{\rm c.m.},J,B)\, dB. \qquad (10)$$

### C. Survival probability of the excited compound nucleus

The survival probability of the excited compound nucleus in the deexcitation process by means of neutron evaporation in competition with fission is expressed as

$$W_{\rm sur}(E^*_{\rm CN},x,J) = F(E^*_{\rm CN},x,J) \prod_{i=1}^{x} \left[ \frac{\Gamma_n(E_i^*,J)}{\Gamma_n(E_i^*,J)+\Gamma_f(E_i^*,J)} \right]_i, \qquad (11)$$

where $F(E^*_{\rm CN},x,J)$ is the realization probability of the $xn$ channel at the excitation energy $E^*_{\rm CN}$ of the compound nucleus with the angular momentum $J$, $i$ is the index of the evaporation step, and $\Gamma_n$ and $\Gamma_f$ are the partial widths of neutron emission and fission. $E_i^*$ is the excitation energy before evaporating the $i$th neutron, which is obtained by the relation

$$E^*_{i+1} = E^*_i - B^n_i - 2T_i, \qquad (12)$$

with the initial condition $E^*_1 = E^*_{\rm CN}$. $B^n_i$ is the separation energy of the $i$th neutron. The nuclear temperature $T_i$ is given by $E^*_i = aT_i^2 - T_i$ with the level density parameter $a$.

## III. NUMERICAL RESULTS AND DISCUSSIONS

### A. Extraction of survival probabilities from experimental cross sections

Different theories have predicted different location of the stability island of the SHN. However, the location has not yet been proved experimentally. Based on the measured data of the ERCS for SHN, and on the different nuclear tables, we try to estimate the stability tendency towards getting heavier elements in the framework of DNS. Using Eq. (13), one can extract the survival probability from experimental ERCSs $\sigma^{\rm expt}_{xn}(E^*_{\rm CN})$ as

$$W_{xn}(E^*_{\rm CN}) = \sigma^{\rm expt}_{xn}(E^*_{\rm CN})/[\sigma^{\rm cap}(E^*_{\rm CN})\,\sigma^{\rm fus}(E^*_{\rm CN})]. \qquad (13)$$

In Fig. 2 the extracted values of $W_{3n}$ and $W_{4n}$ with Eq. (13) are shown. One finds that $W_{3n}$ and $W_{4n}$ for almost all elements from $Z$=112 to 118 based on FRDM1995 mass tables increase with the proton number. Similar results were obtained by

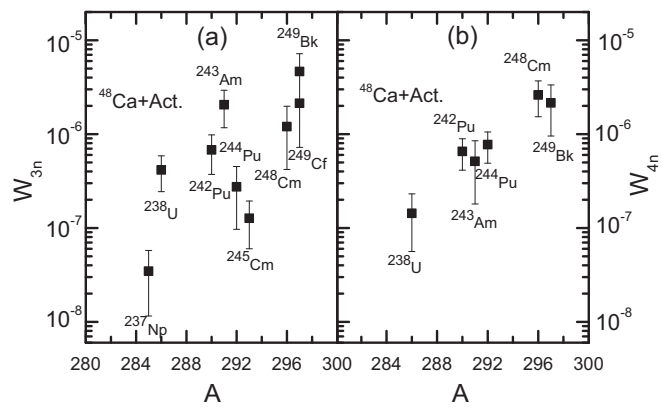


FIG. 2. Survival probabilities of SHN in (a) $3n$ and (b) $4n$ channels, extracted with Eq. (13) and the experimental $\sigma^{\rm expt}_{xn}$ from Refs. [44–49], as functions of mass number of the compound nucleus.

using the KTUY2005 and WS2010 mass tables, indicating an increasing stability of SHN beyond $Z$=114. Therefore, the fission barrier is determined by the shell correction energy, the absolute value of the shell correction energy is expected to be increased with $Z$. This effect has been also illustrated in Ref. [42]. Moreover, the measured $Q_\alpha$ values in $\alpha$-decay chains also indicate the monotonic increase in the region of $Z$=112–118 [43], showing the increasing nuclear stability approaching the closed neutron shell $N$=184. Further, we found that $W_{3n}(^{296}116) < W_{3n}(^{297}118)$. We hope that $Z$=114 is not a proton magic number and that the next spherical doubly magic nucleus beyond $^{208}$Pb is the nucleus with $Z \geqslant 120$. However, the $W_{3n}$ of $^{48}$Ca+$^{249}$Cf does not follow the tendency to go up, but drops down. It is also the same for $W_{4n}(^{296}116) > W_{4n}(^{297}117)$.

In Table I some fission barrier heights from the tables FRDM1995, KTUY2005, WS2010 are shown [26–28]. Note that the fission barrier heights evaluated experimentally in Ref. [50] are the lower limits. One may find that the WS2010 significantly underestimates the barrier heights for all elements from $Z$=112 to 118, while the calculated barrier heights based on the FRDM1995 are in agreement with experimental data. The KTUY2005 predicted higher and increasing barrier heights with $Z$. The fission barrier $B_f$ strongly depends on the neutron and proton numbers of the compound nucleus, especially, on how close they are to the magic numbers. The magic numbers $Z$=114 and $N$=184 are proposed by Möller *et al.* [26]. While Wang *et al.* [27] found the central position of the stability island of SHN may lie at around $N = 176 \sim 178$ and $Z = 116 \sim 120$. The differences among fission barriers evaluated from various approaches increase with $Z$, which become very dramatic for $Z$=120. The biggest differences can reach approximately 3–4 MeV.

TABLE I. Fission barrier heights (in MeV) from different theoretical evaluations: FRDM1995, KTUY2005, WS2010. The experimental data are from Ref. [50].

| Nucleus | FRDM1995 | KTUY2005 | WS2010 | Expt. |
|---|---|---|---|---|
| $^{283}$112 | 6.19 | 5.01 | 4.64 | 5.5 |
| $^{284}$112 | 6.23 | 5.31 | 3.95 | 5.5 |
| $^{285}$112 | 6.63 | 5.66 | 4.09 | 5.5 |
| $^{286}$112 | 6.64 | 5.94 | 4.35 | 5.5 |
| $^{281}$113 | 6.09 | 4.79 | 4.47 | |
| $^{282}$113 | 6.54 | 4.91 | 4.32 | |
| $^{283}$113 | 6.61 | 5.10 | 3.97 | |
| $^{284}$113 | 7 | 5.39 | 4.02 | |
| $^{285}$113 | 7.04 | 5.67 | 4.45 | |
| $^{286}$114 | 7.36 | 6.16 | 5.08 | |
| $^{287}$114 | 7.74 | 6.45 | 4.80 | |
| $^{288}$114 | 7.8 | 6.79 | 5.06 | 6.7 |
| $^{289}$114 | 8.37 | 7.16 | 4.99 | 6.7 |
| $^{290}$114 | 8.61 | 7.59 | 5.07 | 6.7 |
| $^{291}$114 | 8.89 | 8.05 | 5.19 | 6.7 |
| $^{292}$114 | 8.89 | 8.53 | 5.40 | 6.7 |
| $^{287}$115 | 7.76 | 6.44 | 4.93 | |
| $^{288}$115 | 8.16 | 6.70 | 5.04 | |
| $^{289}$115 | 8.17 | 7.02 | 5.27 | |
| $^{290}$115 | 8.52 | 7.38 | 5.16 | |
| $^{291}$115 | 8.66 | 7.79 | 5.31 | |
| $^{289}$116 | 7.83 | 7.07 | 5.41 | |
| $^{290}$116 | 7.81 | 7.34 | 5.60 | |
| $^{291}$116 | 8.07 | 7.64 | 5.44 | |
| $^{292}$116 | 8.3 | 7.98 | 5.60 | 6.4 |
| $^{293}$116 | 8.62 | 8.32 | 5.70 | 6.4 |
| $^{294}$116 | 8.7 | 8.71 | 5.90 | 6.4 |
| $^{295}$116 | 8.98 | 8.86 | 5.53 | 6.4 |
| $^{296}$116 | 8.58 | 9.06 | 5.42 | 6.4 |
| $^{293}$117 | 8.21 | 8.22 | 5.69 | |
| $^{294}$117 | 8.44 | 8.50 | 5.76 | |
| $^{295}$117 | 8.55 | 8.89 | 5.99 | |
| $^{296}$117 | 8.96 | 9.04 | 5.60 | |
| $^{297}$117 | 8.57 | 9.23 | 5.45 | |
| $^{293}$118 | 7.82 | 8.23 | 6.14 | |
| $^{294}$118 | 7.67 | 8.49 | 6.30 | |
| $^{295}$118 | 7.89 | 8.73 | 5.88 | |
| $^{296}$118 | 7.9 | 9.12 | 6.08 | |
| $^{297}$118 | 8.27 | 9.26 | 5.66 | |
| $^{295}$120 | 7.25 | 8.51 | 6.40 | |
| $^{296}$120 | 6.77 | 8.79 | 6.56 | |
| $^{297}$120 | 7.09 | 9.24 | 5.93 | |
| $^{298}$120 | 7.02 | 9.75 | 6.12 | |
| $^{299}$120 | 7.36 | 9.82 | 5.69 | |
| $^{300}$120 | 6.95 | 9.88 | 5.43 | |
| $^{301}$120 | 6.92 | 9.95 | 5.32 | |
| $^{302}$120 | 6.31 | 10.05 | 5.37 | |
| $^{303}$120 | 6.08 | 10.17 | 5.05 | |
| $^{304}$120 | 5.37 | 10.30 | 5.07 | |

### B. Production cross sections of isotopes with $Z$ = 112–118 in $^{48}$Ca-induced reactions

Some ground-state data for the projectile and target nuclei for some fusion channels are listed in Table II. The first and second columns denote the reaction channels and the ground-state deformation of target nuclei, respectively. The third column is the binding energies of target and compound nuclei. The calculated $Q$ values are listed in the last column.

Now we investigate how the data from different tables influence each step to form SHN. The investigation is carried out for $^{48}$Ca+$^{243}$Am based on the data from three the tables: KTUY2005, FRDM1995, and WS2010. Figure 3(a) shows the capture cross section $\sigma_{\rm cap}$ as a function of the excitation energy of the compound nucleus. It is found that the behaviors of the $\sigma_{\rm cap}$ based on the data from KTUY2005 and WS2010 are consistent with each other, while the one based on FRDM1995 is lower. The reason is that data from KTUY2005 and WS2010 provided the same $Q$ value for the reaction $^{48}$Ca+$^{243}$Am, but the FRDM1995 less. The three lines meet together when the excitation energy is approximatively larger than 30 MeV. The fusion probability $P_{\rm CN}$ from different data tables are shown in Fig. 3(b). The PESs for the three cases are shown in Fig. 1. We found the inner fusion barriers from the KTUY2005, FRDM1995, and WS2010 are 11.305, 10.661, and 10.133 MeV, respectively. The competition between fusion and quasifission is taken into account in the fusion probability. The inner fusion barrier hinders the fusion, and the lower surface of the potential energy towards the mass symmetric

TABLE II. Ground-state data for hot fusion reactions to synthesize SHNs: the ground-state deformation, binding energies of target and compound nucleus, and $Q$ value. Those taken from the data tables KTUY2005, FRDM95, and WS2010 are listed in the successive rows for each channel.

| Reaction | g.s. deformation | g.s. binding energies | $Q$ value (MeV) |
|---|---|---|---|
| $^{48}$Ca+$^{238}$U | (0.129) | (−1802.330, −2055.271) | − 163.130 |
| | (0.215) | (−1801.250, −2058.570) | − 158.250 |
| | (0.212) | (−1801.971, −2056.287) | − 161.829 |
| $^{48}$Ca+$^{237}$Np | (0.126) | (−1795.516, −2043.917) | − 167.670 |
| | (0.215) | (−1794.836, −2048.187) | − 162.220 |
| | (0.209) | (−1794.937, −2045.231) | − 165.851 |
| $^{48}$Ca+$^{242}$Pu | (0.137) | (−1825.291, −2074.512) | − 166.850 |
| | (0.224) | (−1824.751, −2078.371) | − 161.950 |
| | (0.221) | (−1825.172, −2074.836) | − 166.481 |
| $^{48}$Ca+$^{244}$Pu | (0.142) | (−1836.394, −2087.725) | − 164.740 |
| | (0.224) | (−1835.903, −2090.754) | − 160.720 |
| | (0.217) | (−1836.470, −2087.476) | − 165.138 |
| $^{48}$Ca+$^{243}$Am | (0.140) | (−1829.710, −2075.981) | − 169.800 |
| | (0.224) | (−1829.510, −2079.840) | − 165.240 |
| | (0.224) | (−1829.812, −2076.324) | − 169.633 |
| $^{48}$Ca+$^{245}$Cm | (0.142) | (−1840.850, −2084.991) | − 171.930 |
| | (0.234) | (−1841.180, −2088.411) | − 168.340 |
| | (0.224) | (−1841.316, −2085.241) | − 172.220 |
| $^{48}$Ca+$^{248}$Cm | (0.144) | (−1858.995, −2105.516) | − 169.550 |
| | (0.235) | (−1859.284, −2107.945) | − 166.910 |
| | (0.227) | (−1859.580, −2104.798) | − 170.927 |
| $^{48}$Ca+$^{249}$Bk | (0.147) | (−1863.294, −2106.875) | − 172.490 |
| | (0.235) | (−1864.073, −2109.284) | − 170.360 |
| | (0.229) | (−1864.070, −2106.074) | − 174.142 |
| $^{48}$Ca+$^{249}$Cf | (0.143) | (−1862.341, −2102.272) | − 176.140 |
| | (0.235) | (−1863.371, −2104.602) | − 174.340 |
| | (0.229) | (−1863.110, −2101.556) | − 177.699 |

region is in favor of quasifission. In the lower excitation energy region $E^*_{CN} < 30$ MeV, and in the WS2010 case the lowest inner fusion barrier gives the highest fusion probability. In the KTUY2005 case, the high inner fusion barrier is not in favor of fusion, but, the higher potential energy surface in the symmetric region is not in favor of quasifission, it gives a relatively moderate fusion probability. When the increasing excitation energy is beyond 30 MeV, the differences among the potentials become less important, the fusion probabilities tend to be all consistent. The survival probabilities are shown in Fig. 3(c). To evaluate the survival probability, very important factors are the fission barrier and neutron separation energy. Based on the data from FRDM1995, $W_{sur}$ is the largest.

Finally, using the above calculated $\sigma_{cap}$, $P_{CN}$, and $W_{sur}$, the ERCSs are obtained and shown in Fig. 4, and the experimental data are also shown for comparison. The measured ERCSs of the 3$n$ and 4$n$ channels are denoted by red open circles and blue solid squares, respectively [47]. The curves for 3$n$ (red lines), 4$n$ (blue lines), and 5$n$ channels (dark cyan lines) are based on the tables of KTUY2005 (solid lines), FRDM1995 (dashed lines), and WS2010 (dashed-dotted lines), respectively. One finds that for the 3$n$ channel the dashed line (FRDM1995)

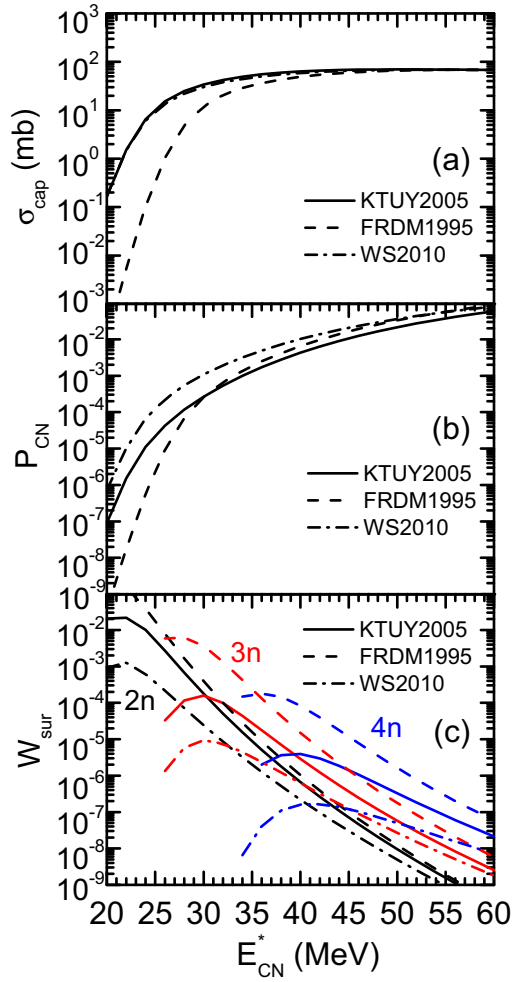


FIG. 3. (Color online) Based on the nuclear tables KTUY2005, FRDM1995, and WS2010, for $^{48}$Ca + $^{243}$Am there are shown (a) capture cross sections, (b) fusion probabilities, and (c) survival probabilities as functions of the excitation energy.

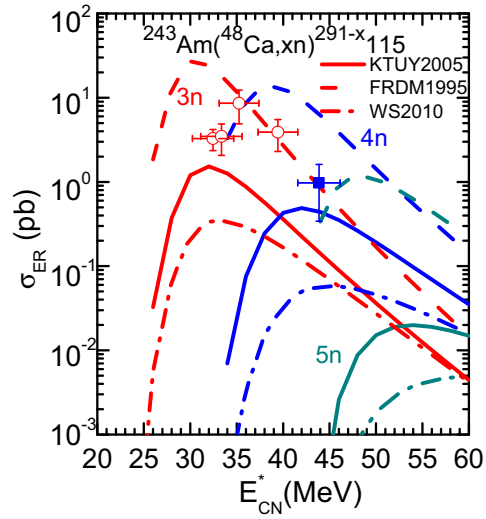


FIG. 4. (Color online) Calculated evaporation residue excitation functions based on the different nuclear tables, compared with the available experimental data [46] for the reaction $^{48}$Ca+$^{243}$Am.

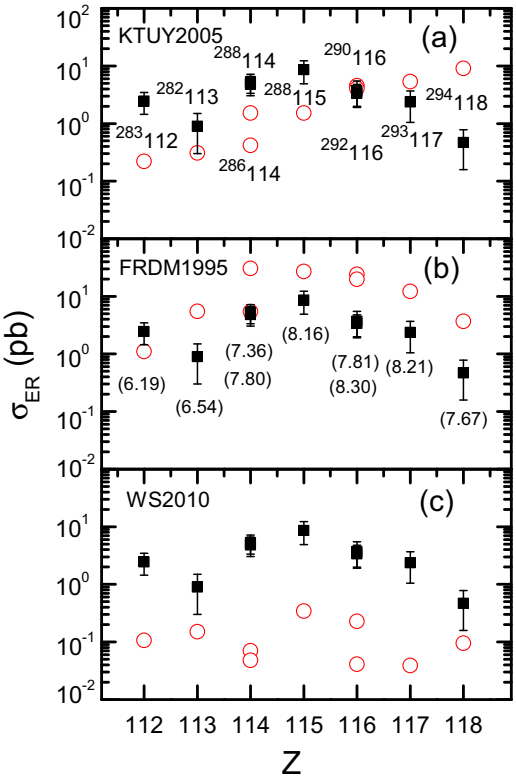


FIG. 5. (Color online) Maximal values of experimentally available ERCSs for $^{48}$Ca-induced reactions [44–49] leading to SHN with $Z$ = 112–118, compared with the theoretical values. For each superheavy nucleus, the charge and mass numbers are given in (a), and they are the same in (b) and (c). The experimental values are shown by black solid squares with error bars and the theoretical ones by red open circles.

is closer to the data, and for the 4$n$ channel the solid line (KTUY2005) is closer to the data. Actually, within the error bars, the experimental data are reasonably reproduced. Theoretical results of the ERCSs are greater than those from experimental data by FRDM1995 table. Furthermore, the predicted positions of the maxima $xn$ excitation functions are shifted by some 3–5 MeV towards lower energies as compared with the experimental data. This effect is also illustrated in Ref. [51], where they used the nuclear table from a microscopic-macroscopic model of the Warsaw Group [52,53].

In Fig. 5, the experimentally obtained maximal ERCSs for $^{48}$Ca-induced reactions leading to SHN with $Z$=112–118 are shown by black square with error bars in each panel. The calculated ones (by open circles) based on different nuclear tables are shown in different panels. For each SHN, the charge and mass numbers are indicated in Fig. 5(a), and they the same for Figs. 5(b) and 5(c). Note that different tables predict different atomic masses and magic numbers in the SHN region. Very different values of ERCSs by applying the various tables are shown. The maximal difference is as large as 3 orders of magnitude. We see generally increasing $\sigma_{\rm ER}$ with $Z$ by the table KTUY2005, underestimated $\sigma_{\rm ER}$ by the table WS2010, and overestimated $\sigma_{\rm ER}$ by the table FRDM1995, but which tends with $Z$ to be very consistent with experimental data. The ERCSs for $^{48}$Ca-induced reactions are usually measured in 3$n$ and 4$n$ channels. From Fig. 3 one may find that when $E^*_{\rm CN} > 30$ MeV, which is the range for excitation energy available to evaporate three and four neutrons as indicated in the figure, there is not much difference for $\sigma_{\rm cap}$ and $P_{\rm CN}$, but there is for $W_{\rm sur}$. Therefore, the differences of the ERCS based on the different tables mainly results from the differences of $W_{\rm sur}$. And the fatal factors for $W_{\rm sur}$ are the neutron separation energy $B_n$ and the fission barrier $B_f$ of the decaying nucleus. Figure 6 shows the $B_n$ and $B_f$ from 3$n$, 4$n$ channels of $^{48}$Ca-induced and synthesized decaying SHNs. The nuclei indicated in the figure are the corresponding target nuclei. It is shown that for the 3$n$,4 $n$ channels of all reactions, no distinct difference is observed for $B_n$, of which the maximal differences is 0.4 MeV among the three tables. However, from the different tables, the predicted fission barriers $B_f$ are quite different, and the range of the difference is about 1–2.5 MeV for the isotopes of SHN with $Z > 112$. Therefore $B_f$ is the fatal factor for the magnitude of the $\sigma_{\rm ER}$. The fission barriers for nuclei shown in Fig. 5 from the table FRDM1995 are indicated below or above the corresponding nuclei in brackets in the middle panel. For the data, we see good correspondence that bigger $B_f$ gives bigger $W_{\rm sur}$, and results in a bigger $\sigma_{\rm ER}$. From Table I, we know that the $B_f$ of various isotope chain out of the FRDM1995 table followed the predicted magic number $Z$=114, and $N$=184. The magnitude of $B_f$ is not only dependent on how close the atomic number of a nucleus is to 114, but also on how close the neutron number of a nucleus is to 184. Therefore the $B_f$ = 8.16 MeV of the nucleus $^{288}$115 is larger than that of $^{286,288}$114, which are 7.36 and 7.80 MeV, respectively, and $\sigma_{\rm ER}(115) > \sigma_{\rm ER}(114)$. On the whole, from $Z$=112–118 the magnitude tendency of the measured $\sigma_{\rm ER}$ as a function of the atomic number $Z$ followed the magnitude tendency of $B_f$ predicted by the table FRDM1995. The most striking thing is that for table KTUY2005, which predicted the magic number $Z$=120, the calculated $\sigma_{\rm ER}$ for $^{294}$118 is much larger. Moreover, for the $Z$=120 isotope chain by FRDM1995, the $B_f$ in Table I is basically decreasing with increasing neutron number, even for $^{304}$120, whose $N$=184.

By using the table FRDM1995, our calculated $\sigma_{\rm ER}$ based on the DNS concept has overestimated the data, but the tendency is very consistent with the data. Recently we further developed the DNS concept so as to have considered the dynamical deformation during the reaction processes [54], and the agreement has improved.

### C. Production cross sections of $Z$ = 120

All three tables have predicted certain fission barriers for the element 120, we thus try to investigate the ERCSs of the yet unexplored new elements $Z$=120. The $^{50}$Ti-induced reaction $^{50}$Ti+$^{249}$Cf and $^{54}$Cr-induced reaction $^{54}$Cr+$^{248}$Cm are studied. The excitation functions of the ERCS are shown in Figs. 7(a) and 7(b) by using KTUY2005 and FRDM1995 tables. With FRDM1995 in both reactions the 3$n$-emission channel gives larger ERCSs than those by the 4$n$ channel. The 3$n$ and 4$n$ channel ERCSs from $^{50}$Ti+$^{249}$Cf are 0.186 and 0.012 pb, respectively, while from the $^{54}$Cr+$^{248}$Cm they are

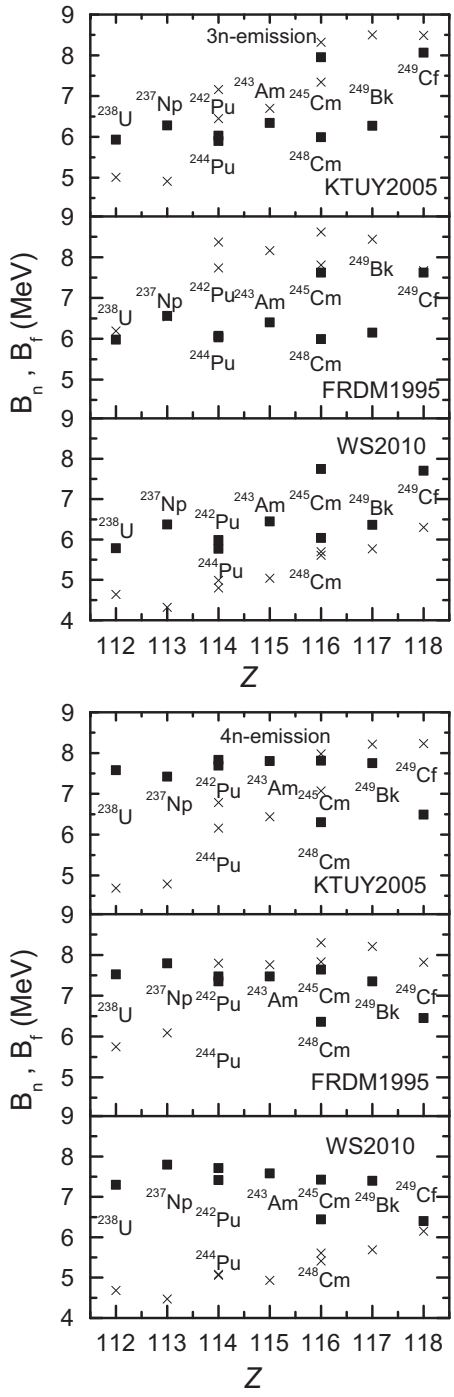


FIG. 6. Neutron binding energies (solid squares) and fission barriers (crosses) predicted with the data of KTUY2005 (upper part), FRDM1995 (middle part), and WS2010 (lower part) for decaying nuclei produced by $^{48}$Ca-induced reactions with the indicated targets for 3$n$ emission and 4$n$ emission.

0.062 and 0.014pb, respectively. The $^{50}$Ti+$^{249}$Cf reaction is more favorable in producing the element $Z$=120. The upper limit of the predicted value is achievable for current experimental conditions. We are aware that the results of our calculations are similar to those predicted by Zagrebaev and Greiner [18] except that our maximum ER cross section in the *3n* channel

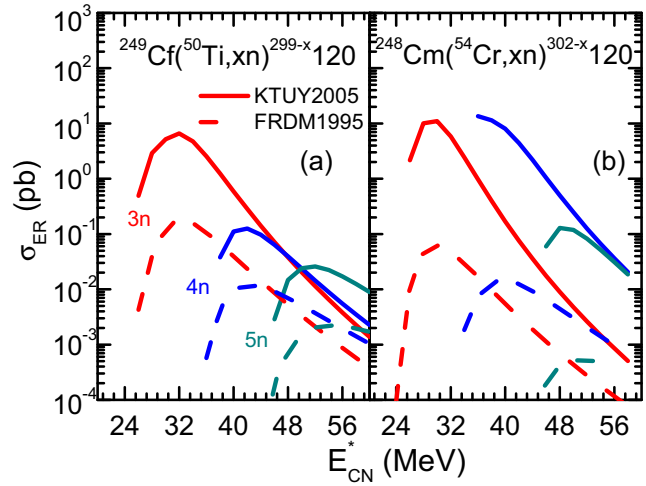


FIG. 7. (Color online) ERCSs of yet undiscovered superheavy nuclei of $Z = 120$ based on KTUY2005 (solid lines) and FRDM1995 (dashed lines).

of the $^{50}$Ti+$^{249}$Cf and $^{54}$Cr+$^{248}$Cm reactions is about two times larger than their results. Similar results were found by Liu and Bao [55] using the table FRDM1995. The results are also similar to those by Nasirov *et al.* [56]. They predicted that the maximum values of ERCS in the 3$n$ channel for the systems $^{50}$Ti+$^{249}$Cf and $^{54}$Cr+$^{248}$Cm are about 0.1 and 0.07 pb, respectively, but the yield of the 4$n$ channel for the former reaction is lower (0.004 pb) as compared with the one (0.01pb) for the latter reaction. With table KTUY2005 the calculated maximum evaporation residue cross sections from $^{249}$Cf($^{50}$Ti, 3$n$)$^{296}$120 and $^{248}$Cm($^{54}$Cr, 3$n$)$^{299}$120 are 6.57 and 11.03 pb for the channel of 3$n$ emission. However, the latest experiment for searching element 120 does not support the result. We are inclined to believe the prediction of $Z = 114$ and $N = 184$ by the FRDM about the magic numbers next to those of $^{208}$Pb; so far the experimental results show no contradictions.

## IV. SUMMARY

Many theories are being carried out to understand the synthesizing mechanism of SHN. However, all of them have to use some basic nuclear data. Based on the DNS concept, and on three data tables (FRDM1995, KTUY2005, and WS2010), the ERCSs of SHN for $Z$=112–118 were calculated for the $^{48}$Ca-induced hot fusion reactions. One can find a generally increasing $\sigma_{ER}$ with $Z$ by table KTUY2005, underestimated $\sigma_{ER}$ by table WS2010, and overestimated $\sigma_{ER}$ by the table FRDM1995, but which all together tend with $Z$ very consistent with data. This is a very prominent characteristic that other tables do not give. Especially, the magnitude of $\sigma_{ER}$ of element 118 is great than that of element 117 by table KTUY2005 and WS2010, the tendency is opposite with that from the data, because the two tables have predicted the magic number $Z$=120. As a consequence, the calculated maximum $\sigma_{ER}$ of element 120 from $^{50}$Ti+$^{249}$Cf are 0.186 and 0.012 pb for 3$n$ and 4$n$ channel, respectively, while from the $^{54}$Cr+$^{248}$Cm are 0.062 and 0.014 pb by FRDM1995. The calculated maximum $\sigma_{ER}$ from $^{249}$Cf($^{50}$Ti, 3$n$)$^{296}$120 and $^{248}$Cm($^{54}$Cr, 3$n$)$^{299}$120 are

6.57 and 11.03 pb for the channel of 3*n* emission by using table KTUY2005. The latest experiments from Dubna, as well as in GSI for searching element 120 do not support the result. It seems that so far the results from the prediction of FRDM have not shown any contradiction with the measured data. In order to reach the SHN with the magic numbers it seems that it is necessary to use the very neutron rich radioactive projectile or/and target.

## ACKNOWLEDGMENTS

Li is grateful for the discussions with Jieding Zhu. The work is supported by the National Natural Science Foundation of China (Grants 11175074, 11475050, and 11265013), the Fundamental Research Funds for the Central Universities (Grantlzujbky-2014-230), by the CAS Knowledge Innovation Project No. KJCX2-EW-N02.

[1] U. Mosel and W. Greiner, Z. Phys. **222**, 261 (1969).
[2] S. G. Nilsson, C. F. Tsang, A. Sobiczewski, Z. Szymanski, S. Wycech, C. Gustafson, I.-L. Lamm, P. Möller, and B. Nilsson, Nucl. Phys. A **131**, 1 (1969).
[3] M. Bender *et al.*, Phys. Lett. B **515**, 42 (2001).
[4] P. Ring, Prog. Part. Nucl. Phys. **37**, 193 (1996).
[5] S. Cwiok *et al.*, Nucl. Phys. A **611**, 211 (1996).
[6] S. Hofmann and G. Münzenberg, Rev. Mod. Phys. **72**, 733 (2000).
[7] S. Hofmann, Radiochim. Acta **99**, 405 (2011).
[8] K. Morita *et al.*, J. Phys. Soc. Jpn. **76**, 045001 (2007).
[9] Y. T. Oganessian, J. Phys. G: Nucl. Part. Phys. **34**, R165 (2007).
[10] Y. T. Oganessian *et al.*, Phys. Rev. Lett. **104**, 142502 (2010).
[11] Y. T. Oganessian, Radiochim. Acta **99**, 429 (2011).
[12] W. J. Swiatecki, Prog. Part. Nucl. Phys. **4**, 383 (1980).
[13] Y. Aritomo, T. Wada, M. Ohta, and Y. Abe, Phys. Rev. C **59**, 796 (1999).
[14] C. W. Shen, Y. Abe, D. Boilley, G. Kosenko, and E. G. Zhao, Int. J. Mod. Phys. E **17**, 66 (2008).
[15] V. I. Zagrebaev, Phys. Rev. C **64**, 034606 (2001).
[16] G. G. Adamian *et al.*, Nucl. Phys. A **627**, 361 (1997); **633**, 409 (1998).
[17] Z. Q. Feng, G. M. Jin, F. Fu, and J. Q. Li, Nucl. Phys. A **771**, 50 (2006).
[18] V. Zagrebaev and W. Greiner, Phys. Rev. C **78**, 034610 (2008).
[19] R. Smolańczuk, Phys. Rev. C **81**, 067602 (2010).
[20] N. Wang, J. Tian, and W. Scheid, Phys. Rev. C **84**, 061601(R) (2011).
[21] Long Zhu, Wen Jie Xie, and Feng-Shou Zhang, Phys. Rev. C **89**, 024615 (2014).
[22] Z. Q. Feng, G. M. Jin, J. Q. Li, and W. Scheid, Phys. Rev. C **76**, 044606 (2007).
[23] N. Wang, E. G. Zhao, W. Scheid, and S. G. Zhou, Phys. Rev. C **85**, 041601(R) (2012).
[24] G. Mandaglio, G. Giardina, A. K. Nasirov, and A. Sobiczewski, Phys. Rev. C **86**, 064607 (2012).
[25] R. K. Choudhury and Y. K. Gupta, Phys. Lett. B **731**, 168 (2014).
[26] P. Möller, J. Nix, W. Myers, and W. Swiatecki, At. Data Nucl. Data Tables **59**, 185 (1995).
[27] Ning Wang, Zuoying Liang, Min Liu, and Xizhen Wu, Phys. Rev. C **82**, 044304 (2010).
[28] H. Koura, T. Tachibana, M. Uno, and M. Yamada, Prog. Theor. Phys. **113**, 305 (2005).
[29] Adam Sobiczewski, and Yuri A. Litvinov, Phys. Rev. C **89**, 024311 (2014).
[30] W. Li, N. Wang, F. Jia, H. Xu, W. Zuo, Q. Li, E. Zhao, J. Li, and W. Scheid, J. Phys. G: Nucl. Phys. **32**, 1143 (2006).
[31] N. Antonenko, E. Cherepanov, A. Nasirov, V. Permjakov, and V. Volkov, Phys. Lett. B **319**, 425 (1993).
[32] N. V. Antonenko, E. A. Cherepanov, A. K. Nasirov, V. P. Permjakov, and V. V. Volkov, Phys. Rev. C **51**, 2635 (1995).
[33] A. S. Zubov, G. G. Adamian, N. V. Antonenko, S. P. Ivanova, and W. Scheid, Phys. Rev. C **65**, 024308 (2002).
[34] C. Y. Wong, Phys. Rev. Lett. **31**, 766 (1973).
[35] Z. Q. Feng, G. M. Jin, and J. Q. Li, Phys. Rev. C **80**, 057601 (2009).
[36] M. H. Huang *et al.*, Chin. Phys. Lett. **25**, 1243 (2008).
[37] G. Wolschin and W. Nörenberg, Z. Phys. A **284**, 209 (1978).
[38] J. Q. Li and G. Wolschin, Phys. Rev. C **27**, 590 (1983).
[39] P. Grange, Li Jun-Qing, and H. A. Weidenmuller, Phys. Rev. C **27**, 2063 (1983).
[40] G. G. Adamian, N. V. Antonenko, and W. Scheid, Phys. Rev. C **68**, 034601 (2003).
[41] G. G. Adamian, N. V. Antonenko, R. V. Jolos, S. P. Ivanova, and O. I. Melnikova, Int. J. Mod. Phys. E **5**, 191 (1996).
[42] G. G. Adamian, N. V. Antonenko, and V. V. Sargsyan, Phys. Rev. C **79**, 054608 (2009).
[43] S. Hofmann *et al.*, Eur. Phys. J. A **32**, 251 (2007).
[44] Y. T. Oganessian *et al.*, Phys. Rev. C **70**, 064609 (2004).
[45] Y. T. Oganessian *et al.*, Phys. Rev. C **76**, 011601(R) (2007).
[46] Y. T. Oganessian *et al.*, Phys. Rev. C **69**, 054607 (2004).
[47] Y. T. Oganessian *et al.*, Phys. Rev. C **87**, 014302 (2013).
[48] Y. T. Oganessian *et al.*, Phys. Rev. C **74**, 044602 (2006).
[49] Y. T. Oganessian *et al.*, Phys. Rev. C **87**, 054621 (2013).
[50] M. G. Itkis, Yu. Ts. Oganessian, and V. I. Zagrebaev, Phys. Rev. C **65**, 044602 (2002).
[51] K. Siwek-Wilczyńska, T. Cap, M. Kowal, A. Sobiczewski, and J. Wilczyński, Phys. Rev. C **86**, 014611 (2012).
[52] I. Muntian, Z. Patyk, and A. Sobiczewski, Phys. At. Nucl. **66**, 1015 (2003).
[53] M. Kowal, P. Jachimowicz, and A. Sobiczewski, Phys. Rev. C **82**, 014303 (2010).
[54] X. J. Bao, Y. Gao, J. Q. Li, and H. F. Zhang, Phys. Rev. C **91**, 011603(R) (2015).
[55] Zu-Hua Liu and Jing-Dong Bao, Phys. Rev. C **87**, 034616 (2013).
[56] A. K. Nasirov, G. Mandaglio, G. Giardina, A. Sobiczewski, and A. I. Muminov, Phys. Rev. C **84**, 044612 (2011).